

Dynamic magnetostriction for antiferromagnets

Thomas Nussle*

*CEA DAM/Le Ripault, Boîte Postale 16, F-37260 Monts, France**and Institut Denis Poisson, Université de Tours, Université d'Orléans, CNRS (UMR7013), Parc de Grandmont, F-37200 Tours, France*Pascal Thibaudeau[†]*CEA DAM/Le Ripault, Boîte Postale 16, F-37260 Monts, France*Stam Nicolis[‡]*Institut Denis Poisson, Université de Tours, Université d'Orléans, CNRS (UMR7013), Parc de Grandmont, F-37200 Tours, France*

(Received 28 June 2019; revised manuscript received 7 November 2019; published 23 December 2019)

In this paper, we study the switching properties of the dynamics of magnetic moments that interact with an elastic medium. To do so, we construct a Hamiltonian framework that can take into account the dynamics in phase space of the variables that describe the magnetic moments in a consistent way. It is convenient to describe the magnetic moments as bilinears of anticommuting variables that are their own conjugates. However, we show how it is possible to avoid having to deal directly with the anticommuting variables themselves, only using them to deduce nontrivial constraints on the magnetoelastic couplings. We construct the appropriate Poisson bracket and a geometric integration scheme that is symplectic in the extended phase space and that allows us to study the switching properties of the magnetization, which are relevant for applications, for the case of a toy model for antiferromagnetic NiO, under external stresses. In the absence of magnetoelastic coupling, we recover the results reported in the literature and in our previous studies. In the presence of the magnetoelastic coupling, the characteristic oscillations of the mechanical system have repercussions on the Néel order parameter dynamics. This is particularly striking for the spin accumulation, which is more than doubled by the coupling to the strain; here as well, the mechanical oscillations are reflected on the magnetic dynamics. As a consequence of such a stress-induced strain, the switching time of the magnetization is slightly faster, and the amplitude of the magnetization is enhanced.

DOI: [10.1103/PhysRevB.100.214428](https://doi.org/10.1103/PhysRevB.100.214428)**I. INTRODUCTION**

With the emergence of spintronics, attention has now been focused on the theoretical understanding and experimental manipulation of the properties of magnetic materials at ever shorter length and time scales. In this context, antiferromagnets (AFs) are the magnetically ordered materials that appear to be among the most promising candidates for realizing fast spintronic devices with very low power consumption [1]. Therefore, quantitative modeling of spin transport is also of topical interest.

Recent progress in describing spin transport and spin-transfer torque (STT) effects in such AF devices has paved the way toward developing multilevel memory devices with switching speeds, which could exceed those of devices made of ferromagnetic materials and semiconductors [2]. Moreover, reversible strain-induced magnetization switching in ferromagnetic materials has been reported that also allows the design of a rewritable, nonvolatile, nontoggle, and extremely

low-energy straintronic memory [3]. Recently, a piezoelectric, strain-controlled AF memory, insensitive to magnetic fields, has been tested as an example of controlling magnetism by electric fields in multiferroic heterostructures [4].

However, a theoretical description of all these phenomena is still very much a work in progress since at the scales that are relevant, it is not possible to separate the magnetic, electric, and elastic responses—all must be treated simultaneously.

It is indeed noteworthy that no direct local coupling between electromagnetic field components is allowed in vacuum at the classical level; the magnetic response to an electric field is necessarily mediated by atomic position arrangements of magnetic moments, which in response produce nonlocal mechanical strains [5,6]. This response is known, more generally, under the heading of “magnetoelasticity” [7].

Magnetoelastic phenomena have been typically viewed either from the perspective of continuum mechanics, where the magnetic properties of materials are incorporated into constitutive nonlinear laws of electroconductive bodies [8], or through the introduction of effective magnetic anisotropies mimicking the static strains of a solid [9].

Most studies, however, do not investigate the backreaction of the magnetization on the mechanical strains; however, such a backreaction can become significant at very short length and

*thomas.nussle@cea.fr

†pascal.thibaudeau@cea.fr

‡stam.nicolis@lmpt.univ-tours.fr

time scales (where a continuum description reaches its limits). This highlights the need for developing multiscale models.

Even if multiscale models have been investigated for magnetoelastic couplings [10], with good experimental comparison for single crystals and polycrystalline samples [11], insights from the framework of localization and homogenization are still the mainstay for deducing the constitutive laws for polycrystalline media. Moreover, in this context, homogenization methods for multiscale mechanics assume the existence of well-separated scales and different relations among length scales that lead to different effective equations, which in turn represent the corresponding different physical effects appropriate at each scale [12].

Renormalization-group ideas, of course, are instrumental in providing a description of how the dynamics depends on the scale; what has been lacking to date is a unified construction of the dynamics of elastic and spin degrees of freedom within a common Hamiltonian approach at any particular scale. In particular, what has curiously not been fully exploited is the resolution of the constraints to which the spin degrees of freedom are subject, since they are their own canonically conjugate variables, as their equations of motion are first-order. This means that they can be most usefully expressed as multilinear combinations of *anticommuting* variables. As we shall see, this can lead to useful insights, in practice, about the dynamics of the coupled system.

While the generalization of the canonical formalism that incorporates the constraints implied by spin degrees of freedom was worked out a long time ago [13], it has not been applied to concrete situations of physical interest, simply because up to now these were not of practical relevance.

In the present paper, we provide a complete description of the combined Hamiltonian dynamics of the elastic and of the spin degrees of freedom in phase space, and we show how the anticommuting nature of the spin degrees of freedom can be indirectly tested. It is the refined control over these and the dynamical interplay between strain and magnetization that are the particular novelties of our approach.

The elastic (local mechanical strain) and spin degrees of freedom are thus assigned to sites of a lattice. We deduce the corresponding fully coupled equations of motion from the corresponding Hamiltonian formalism, which treats mechanical and spin degrees of freedom in a unified way, and we study the dynamics of this system, comparing it to previous studies, first for the purely magnetic part [14] and then also for the magnetoelastically coupled system [15].

Of course, to render the equations tractable we must resort to approximations. The approximation we employ is the mean-field approximation, which amounts, in the present case, to a coarse-graining of the lattice, which means that the sites are, in fact, domains within each of which the properties are homogeneous. Within this framework, our Hamiltonian formalism is, however, exact.

The paper is organized as follows: In Sec. II we construct a classical Hamiltonian for the mechanical and the spin degrees of freedom and we discuss their couplings. We discuss the advantages of describing the magnetic moments in terms of anticommuting, Majorana, variables, whose salient properties are reviewed in Appendix A.

In Sec. III, we introduce a Poisson bracket, which allows us to obtain the equations of motion for the time evolution of all the dynamical variables. These are then solved in Sec. IV using a symplectic integration scheme. Special attention is devoted to the stability analysis of the schemes and to the order of the different symplectic operators. This analysis is presented in Appendix B.

Finally, in Sec. V we illustrate the formalism for the case of a simple toy model for NiO, consisting of two spins, interacting through antiferromagnetic exchange, and switched by an external STT as well as under an external stress. It is here, in particular, that we show that the formalism is capable of handling the interaction between two domains, taking into account the coupling between elastic and magnetic degrees of freedom.

II. THE HAMILTONIAN

In this section, we propose a Hamiltonian for the combined system of elastic and spin degrees of freedom. These parts have obviously been considered before [7], so we shall review the salient features before introducing our approach.

The starting point for the elastic degrees of freedom is the framework of mechanics for elastic solids within the regime of the approximation of small deformations supplemented by the assumption of perfect mechanical microreversibility [16]. These statements imply that an elastic material is characterized by a collection of N time-dependant elastic deformations, which are described by a set of symmetric Cauchy strain tensors $\epsilon_{IJ}^i(t)$, where I, J are spatial indices ranging from 1 to 3 and assigned to each lattice site, $i \in \{1, \dots, N\}$, of the material. At equilibrium, each of these variables is independent of time, and we assume that such a state not only exists but can be relevant for the time scales of interest [8].

The total internal energy of this system can be described in terms of the interactions between these variables, which take into account the elastic mechanical part in the most general form, and the interaction with external stresses, which will be described by the magnetic degrees of freedom. Schematically,

$$\frac{\mathcal{H}}{V_0} = \frac{\mathcal{H}_{\text{mech}}}{V_0} + \frac{\mathcal{H}_{\text{ext}}}{V_0}. \quad (1)$$

We shall now spell out each term.

To lowest nontrivial, i.e., quadratic order, $\mathcal{H}_{\text{ext}}/V_0$ can be written as [17]

$$\frac{\mathcal{H}_{\text{mech}}}{V_0} = \frac{1}{2} \sum_{i=1}^N C_{IJKL}^i \epsilon_{IJ}^i(t) \epsilon_{KL}^i(t), \quad (2)$$

where an implicit sum on the repeated space indices is understood and where C_{IJKL}^i are the elastic constants with V_0 as the reference volume.

In this expression, we have assumed that the different sites of the material do not interact through elastic deformations (they will only interact through spin exchange forces, to be explained below).

For a homogeneous material (i.e., $C^{(i)} = C$ for every site i), these elastic constants can be expressed in terms of the two Lamé parameters [16], designated by (C_0, C_1) , which in

Cartesian coordinates read as follows:

$$C_{IJKL} = C_0 \delta_{IJ} \delta_{KL} + C_1 (\delta_{IK} \delta_{JL} + \delta_{IL} \delta_{JK}). \quad (3)$$

This mechanical system can be excited by an external stress σ_{IJ}^{ext} through the coupling

$$\frac{\mathcal{H}_{\text{ext}}}{V_0} = - \sum_{i=1}^N \sigma_{IJ}^{\text{ext}} \epsilon_{JI}^i. \quad (4)$$

While this stress can be, in general, a time- and space-dependent quantity, it is nonetheless assumed to be uniform over the sites of the material.

The magnetic degrees of freedom, denoted $S_i^j(t)$, are assigned to the same lattice sites as the strain and describe how their dynamics affects the mechanical degrees of freedom through the so-called magnetoelastic coupling.

The contribution of the magnetoelastic coupling to the Hamiltonian can be deduced by assuming (global) Galilean invariance on the one hand, and imposing invariance under the symmetries of the point group [18] on the other. For an isotropic medium, these requirements lead to the expressions for the total energy and the total magnetization [19]. The total internal energy is thus a sum over the lattice [20].

Consequently, in the approximation of small deformations, the expansion of the magnetoelastic coupling energy will contain even powers of the magnetization S^j . It will, however, contain all powers of the strain tensor, ϵ .

The linear part in ϵ_{IJ}^i defines the first-order, magnetoelastic coupling, which is responsible for the magnetostriction, while the quadratic terms in ϵ_{IJ}^i define the second-order magnetoelastic coupling, which is responsible for the “nonlinear response” in the elastic properties of magnetic media, which have also been identified as describing “morphic effects” [7].

Higher-order terms are usually ignored since their coefficients are assumed to be much smaller than the lower-order terms, as already discussed.

Therefore, the contribution to the—total—Hamiltonian of the magnetoelastic coupling can be written as

$$\begin{aligned} \mathcal{H}_{\text{ME}} = & \sum_{i,j=1}^N B_{IJKL}^{(1)i,j} \epsilon_{IJ}^i(t) S_K^i(t) S_L^j(t) \\ & + B_{IJKLMN}^{(2)i,j} \epsilon_{IJ}^i(t) \epsilon_{KL}^j(t) S_M^i(t) S_N^j(t) + \dots \end{aligned} \quad (5)$$

The total Hamiltonian can thus be written as

$$\mathcal{H}_{\text{tot}} = \mathcal{H}_{\text{mech}} + \mathcal{H}_{\text{ext}} + \mathcal{H}_{\text{ME}} \quad (6)$$

and leads to a “renormalization” of the effective elastic constants in the following way: If one compares the last term of Eq. (5) with Eq. (2), it is easy to see that a pair of effective elastic constants can be introduced that depends on the value of the spins on each site, i.e.,

$$C_{IJK}^{\text{eff},i,j} \equiv C_{IJK}^{ij} + \frac{1}{V_0} B_{IJKLMN}^{(2)i,j} S_M^i(t) S_N^j(t). \quad (7)$$

This has been used to provide an interpretation of the “anomalous” temperature dependence in the elastic constants in iron single crystals, for instance, as resulting from the competition between spin ordering and diffusion effects [21]. In the present work, however, we will only consider $B_{IJKL}^{(1)i,j}$ and set

aside the nonlinear mechanical terms. Although there is no particular difficulty in taking the latter into account in this formalism, we will take $B^{(2)} \equiv 0$ for the rest of this study and for the sake of simplicity.

In Appendix A, we recall that the most effective “classically equivalent description” of the spin degrees of freedom, which can capture consistently their interaction with the elastic degrees of freedom, is not through the variables S but through their “Doppelgänger” ξ , related to the S_i^j through

$$S_i^j \equiv -\frac{i}{2} \epsilon_{IJK} \xi_J^i \xi_K^j. \quad (8)$$

The ξ can be identified with Majorana fermions, which have found many applications recently in condensed-matter systems [22], where new methods for controlling spin degrees of freedom have been developed.

It is interesting to remark that the anticommuting variables ξ_k^i are not Grassmann variables, satisfying $\{\xi_J^i, \xi_J^j\} = 0$, but rather $\{\xi_J^i, \xi_J^j\} = \delta^{ij} \delta_{JJ}$, i.e., that the ξ_I generate a Clifford algebra on each site [23]. It is in this way that the S_i^j , defined through Eq. (8), satisfies the angular momentum algebra [24].

If one were tempted to simply replace S by ξ in Eq. (5) for $N = 1$, and because of the symmetries of $B^{(1)}$ as recalled in Ref. [7], $\mathcal{H}_{\text{ME}} = 0$, which implies that the dynamics as it is cannot be encoded by this Hamiltonian.

On the other hand, this allows us to understand the constraints on the allowed terms in the true Hamiltonian. They must necessarily involve more than one spin. Indeed, we can construct expressions that are multilinear combinations of the S_i^j on different sites, potentially up to order N , the number of sites, since no two identical ξ_J^i variables occur in the same monomial. This is therefore a nice way of automatically organizing the multispin terms of the Hamiltonian.

In the formalism of atomistic spin dynamics, since the magnetic moments are localized [25,26], it is customary to consider spatial averages around each site defining an effective macroscopic localized spin

$$S_I^{\text{eff}} = \langle S_I^i \rangle, \quad (9)$$

which implies that multilinear expressions $S_I S_J$ no longer vanish identically, as was imposed by the anticommuting nature of ξ before. We can thus understand the relevance of this averaging procedure in terms of the description of the spin degrees of freedom in terms of the anticommuting variables.

The justification for Eq. (5) was advocated a long time ago [27] as stemming from a model for a two-body interaction, which is itself a pedagogical version of the quantum theory of interacting magnons and phonons [28]. In Eq. (5), what has been left unspecified are the properties of the tensor $B^{(1)}$ under exchange of the indices i and j that label the sites. What is customary is to assume that $B^{(1)}$ in fact does not depend on i and j at all—it is homogeneous across the material. By stopping the expansion at first order in the mechanical deformation in (5) and assuming homogeneity in the material, we therefore end up with the following expression:

$$\mathcal{H}_{\text{ME}} = B_{IJKL}^{(1)} \epsilon_{IJ}(t) S_K(t) S_L(t). \quad (10)$$

Again, in the case of an isotropic medium, the elements in $B^{(1)}$ enjoy the same symmetries as the elastic constants and can be expressed only in terms of two constants $B_0^{(1)}$ and $B_1^{(1)}$ by the

following expression:

$$B_{IJKL}^{(1)} = B_0^{(1)} \delta_{IJ} \delta_{KL} + B_1^{(1)} (\delta_{IK} \delta_{JL} + \delta_{IL} \delta_{JK}). \quad (11)$$

In summary, the microscopic theory underlying Eq. (10) describes the interaction of three particles, two of which describe spin states, and one that describes the state of the elastic deformation. However, the spin states are in fact bound states of more “fundamental” entities, the anticommuting ξ . $B^{(1)}$ can then be interpreted as the vertex of this interaction, which describes a spinning particle that does not directly interact with itself, since any such interaction is inconsistent with the fact that the ξ anticommute. Such a self-interaction can, however, appear on larger scales when spatial averages can become meaningful for describing the spin degrees of freedom.

In conclusion, the Hamiltonian we have constructed describes the interaction of magnetic moments through their embedding within an elastic medium. What remains to be done is to define the Poisson brackets, which can take into account the evolution in phase space of commuting as well as anticommuting degrees of freedom. Indeed, the construction procedure for commuting canonical variables is well known, however including anticommuting variables in a unified way has remained a rather esoteric subject—known in theory [13], but not implemented in practice.

In the following section, we shall construct the equations of motion in the phase space of the elastic and the spinning degrees of freedom, which implements these ideas in practice.

To work directly with the anticommuting variables themselves in combination with the mechanical degrees of freedom requires implementing a graded Poisson bracket; one way to do this is discussed in Appendix A.

III. THE POISSON BRACKETS AND THE EQUATIONS OF MOTION

To deduce the equations of motion from the Hamiltonian discussed in the previous section, we must define the appropriate pairs of canonically conjugate variables and consequently their Poisson bracket.

First we recognize that ε acts as a tensor, and one can understand the definition of the Poisson bracket of rank-2 symmetric tensors as an application of the DeDonder-Weyl covariant Hamiltonian formulation of field theory [29]. Although the context is different, the ADM procedure in general relativity also provides such a Poisson bracket [30] (with further relations between the conjugate variables that are not relevant here).

Although no clear consensus has in fact emerged on the properties of the Poisson bracket of rank-2 tensors [31], if one focuses on the special case of strain tensors that depend only on time, the following conjugate momentum can be introduced:

$$\pi_{IJ} \equiv \frac{\partial \mathcal{L}}{\partial \dot{\varepsilon}_{IJ}}, \quad (12)$$

where $\mathcal{L}(\varepsilon_{IJ}(t), \dot{\varepsilon}_{IJ}(t))$ is the unconstrained and free Lagrangian. $\dot{\varepsilon}_{IJ}(t)$ are the components of the strain-rate tensor [32].

Thus we can build the corresponding Hamiltonian \mathcal{H} for the time evolution with tensor variables for mechanical deformations ε and their conjugated momenta π , because these quantities admit unbounded numerical values, as the corresponding Legendre transform

$$\mathcal{H}(\varepsilon, \pi) = \pi_{IJ} \dot{\varepsilon}_{IJ} - \mathcal{L} \quad (13)$$

up to a total time derivative for \mathcal{L} .

For the mechanical system only [i.e., for functions $A(\varepsilon, \pi)$ and $B(\varepsilon, \pi)$], the Poisson bracket (PB) can be defined in perfect analogy to that of any particle system that explores a given target space geometry (to which the indices I, J, K, L refer) by the usual relations

$$\{A, B\}_{\text{PB}} = \frac{\partial A}{\partial \varepsilon_{IJ}} \frac{\partial B}{\partial \pi_{IJ}} - \frac{\partial A}{\partial \pi_{IJ}} \frac{\partial B}{\partial \varepsilon_{IJ}}. \quad (14)$$

In our case, the dynamical variables are the real symmetric rank-2 tensors, ε_{IJ} and π_{IJ} ($I, J = 1, 2, 3$), which are canonically conjugate in the sense that their Poisson brackets are deemed to satisfy the following properties:

$$\{\varepsilon_{IJ}, \pi_{KL}\}_{\text{PB}} = \delta_{IJKL}, \quad (15)$$

$$\{\varepsilon_{IJ}, \varepsilon_{KL}\}_{\text{PB}} = \{\pi_{IJ}, \pi_{KL}\}_{\text{PB}} = 0, \quad (16)$$

where δ_{IJKL} is a δ multilinear object, reflecting the real, symmetric, nature of the Poisson brackets [33] and defined as a product of Kronecker δ 's. Very schematically, we may write

$$\delta_{IJKL} = \begin{cases} \delta_{IJ} \delta_{KL}, \\ \delta_{IJ} \delta_{LK}, \\ \delta_{JI} \delta_{LK}, \\ \delta_{JI} \delta_{KL}, \end{cases} \quad (17)$$

where each choice of the right-hand side corresponds to a choice of indices in the Poisson brackets. This choice can be supplemented by any linear combination of these δ 's that enforces the symmetries of the tensors.

We now wish to include as phase-space coordinates the components of the spin vector, \mathbf{S} . We follow Ref. [34], and the details are summarized in Appendix A. The Poisson bracket for the canonical variables of our system can be written as

$$\{A, B\}_{\text{PB}} \equiv \frac{\partial A}{\partial \varepsilon_{IJ}} \frac{\partial B}{\partial \pi_{IJ}} - \frac{\partial A}{\partial \pi_{IJ}} \frac{\partial B}{\partial \varepsilon_{IJ}} - \frac{1}{\hbar} \epsilon_{IJK} S_I \frac{\partial A}{\partial S_J} \frac{\partial B}{\partial S_K}, \quad (18)$$

where \hbar is introduced to restore the physical dimensions of the Poisson bracket, since \mathbf{S} is considered dimensionless for the sake of simplicity.

It should be stressed that this \hbar does not imply that any quantum effects are present since the dynamics is fully classical. It is simply a bookkeeping device for a quantity that has the dimensions of angular momentum, i.e., of an area in phase space, and it reflects the fact that the equation of motion for S_I is of first order. Quantum fluctuations will introduce the “real” \hbar .

Using this Poisson bracket, we can obtain the equations of motion for the phase-space variables:

$$\begin{aligned}\dot{\epsilon}_{IJ} &= \{\epsilon_{IJ}, \mathcal{H}\}_{\text{PB}} = \frac{\partial \mathcal{H}}{\partial \pi_{IJ}}, \\ \dot{\pi}_{IJ} &= \{\pi_{IJ}, \mathcal{H}\}_{\text{PB}} = -\frac{\partial \mathcal{H}}{\partial \epsilon_{IJ}}, \\ \dot{S}_I &= \{S_I, \mathcal{H}\}_{\text{PB}} = \frac{1}{\hbar} \epsilon_{IJK} S_J \frac{\partial \mathcal{H}}{\partial S_K}.\end{aligned}\quad (19)$$

The consistency of this formalism can be checked by noting that these equations preserve the volume in phase space,

$$\frac{\partial \dot{\epsilon}_{IJ}}{\partial \epsilon_{IJ}} + \frac{\partial \dot{\pi}_{IJ}}{\partial \pi_{IJ}} + \frac{\partial \dot{S}_K}{\partial S_K} = 0. \quad (20)$$

That the dynamics preserves the volume in phase space does not, of course, imply anything about whether the system thus defined is integrable or shows Hamiltonian chaos.

The internal energy U involving the mechanical energy for the deformed elastic medium [16], the magnetic energy defined by the Zeeman term [35], and the magnetoelastic energy [7] which takes into account the interaction of the magnetic moment with the medium, takes the form

$$U = \frac{V_0}{2} C_{IJKL} \epsilon_{IJ} \epsilon_{KL} - V_0 \sigma_{IJ}^{\text{ext}} \epsilon_{IJ} + B_{IJKL}^{(1)} \epsilon_{IJ} S_K S_L - \hbar \omega_I S_I, \quad (21)$$

where C is the fully symmetric tensor defining the elastic response, σ^{ext} is the external stress tensor, ω is the effective external magnetic field (expressed as a frequency), and $B^{(1)}$ is the fully symmetric linear magnetostriction tensor.

The “kinetic” term, containing the conjugate momenta, can be written schematically as

$$\mathcal{H}_{\text{kinetic}} = \frac{1}{2} \pi_{IJ} M_{IJKL}^{-1} \pi_{KL}, \quad (22)$$

where M is a fully symmetric “mass” matrix that describes the inertial response.

For the case of isotropic materials, it is assumed that the M tensor has the form given by Lamé, with only two characteristic constants:

$$M_{IJKL} = M_0 \delta_{IJ} \delta_{KL} + M_1 (\delta_{IK} \delta_{JL} + \delta_{IL} \delta_{JK}). \quad (23)$$

The tensors C and B are decomposed in the same way.

Consequently, the inverse of these tensors can then be deduced from $M_{IJKL} M_{IJMN}^{-1} = \frac{1}{2} (\delta_{KM} \delta_{LN} + \delta_{KN} \delta_{LM})$. Thus

$$\begin{aligned}M_{IJKL}^{-1} &= \frac{-M_0}{2M_1(3M_0 + 2M_1)} \delta_{IJ} \delta_{KL} \\ &\quad + \frac{1}{4M_1} (\delta_{IK} \delta_{JL} + \delta_{IL} \delta_{JK})\end{aligned}\quad (24)$$

and the equations of motion become

$$\begin{aligned}\dot{\epsilon}_{IJ} &= M_{IJKL}^{-1} \pi_{KL}, \\ \dot{\pi}_{IJ} &= -V_0 C_{IJKL} \epsilon_{KL} + V_0 \sigma_{IJ}^{\text{ext}} - B_{IJKL} S_K S_L, \\ \dot{S}_I &= \epsilon_{IJK} \left(\omega_J - \frac{2}{\hbar} B_{ABJC}^{(1)} \epsilon_{AB} S_C \right) S_K,\end{aligned}\quad (25)$$

highlighting how the mechanical and magnetic subsystems are coupled.

The last equation—as expected—is a precession equation for the components of \mathbf{S} around both the effective field $\boldsymbol{\omega}$ and an additional field, which depends on the strain tensor and the spin vector.

In the following section, we shall show how to solve these equations in a way that preserves the symmetries of the extended phase space.

IV. GEOMETRIC INTEGRATION

Solving the coupled system of Eqs. (25) is the next step.

Since in the previous section we showed that these equations describe a volume-preserving transformation of the enlarged phase space, encompassing elastic *and* spin variables, it is natural to rewrite them in terms of the action of a Liouville operator. Therefore, we shall write Eqs. (25) as

$$\begin{aligned}\dot{\boldsymbol{\epsilon}} &= \mathcal{L}_\epsilon \boldsymbol{\epsilon}, \\ \dot{\boldsymbol{\pi}} &= \mathcal{L}_\pi \boldsymbol{\pi}, \\ \dot{\mathbf{S}} &= \mathcal{L}_S \mathbf{S},\end{aligned}\quad (26)$$

where \mathcal{L} is the Liouville operator. This formulation allows us to implement, manifestly, time-reversible area-preserving algorithms for solving these equations numerically.

The general scheme is as follows: Consider an arbitrary function f of the canonically conjugate variables of our many-body system. This function, $f(\boldsymbol{\epsilon}, \boldsymbol{\pi}, \mathbf{S})$, depends on the time t implicitly, that is, through the dependence of $(\boldsymbol{\epsilon}, \boldsymbol{\pi}, \mathbf{S})$ on t . The time derivative of f is \dot{f} such that

$$\dot{f} = \dot{\epsilon}_{IJ} \frac{\partial f}{\partial \epsilon_{IJ}} + \dot{\pi}_{IJ} \frac{\partial f}{\partial \pi_{IJ}} + \dot{S}_I \frac{\partial f}{\partial S_I} \equiv \mathcal{L}f. \quad (27)$$

The last line defines the (total) Liouville operator

$$\mathcal{L} = \dot{\epsilon}_{IJ} \frac{\partial}{\partial \epsilon_{IJ}} + \dot{\pi}_{IJ} \frac{\partial}{\partial \pi_{IJ}} + \dot{S}_I \frac{\partial}{\partial S_I}. \quad (28)$$

Equation (27) can be integrated formally as an initial value problem to obtain f at any time:

$$f(\boldsymbol{\epsilon}(t), \boldsymbol{\pi}(t), \mathbf{S}(t)) = e^{\mathcal{L}t} f(\boldsymbol{\epsilon}(0), \boldsymbol{\pi}(0), \mathbf{S}(0)). \quad (29)$$

It is not difficult to see that $\mathcal{L} = \mathcal{L}_\epsilon + \mathcal{L}_\pi + \mathcal{L}_S$. However, these single Liouville operators do not commute two-by-two, as the reader may easily check by computing $\mathcal{L}_u \mathcal{L}_v f - \mathcal{L}_v \mathcal{L}_u f \neq 0$ for any function f and any combination (u, v) of the individual Liouville operator $\mathcal{L}_\epsilon, \mathcal{L}_\pi, \mathcal{L}_S$. This means that

$$e^{\mathcal{L}t} = e^{\mathcal{L}_\epsilon t + \mathcal{L}_\pi t + \mathcal{L}_S t} \neq e^{\mathcal{L}_\epsilon t} e^{\mathcal{L}_\pi t} e^{\mathcal{L}_S t}. \quad (30)$$

According to the Magnus expansion [36], however, it is always possible to express $e^{\mathcal{L}t}$ as a product of the individual operators at any given order in time according to the so-called “splitting method” [37]. This ensures that the numerical algorithm preserves phase-space volumes exactly.

For instance, for a fixed time step τ , upon expanding up to the third order in time, the following sequence of products:

$$e^{\mathcal{L}\tau} = e^{\mathcal{L}_S \frac{\tau}{4}} e^{\mathcal{L}_\pi \frac{\tau}{2}} e^{\mathcal{L}_S \frac{\tau}{4}} e^{\mathcal{L}_\epsilon \tau} e^{\mathcal{L}_S \frac{\tau}{4}} e^{\mathcal{L}_\pi \frac{\tau}{2}} e^{\mathcal{L}_S \frac{\tau}{4}} + O(\tau^3), \quad (31)$$

can be generated; this sequence is in fact one of six possible sequences that has the property of preserving the symplectic structure of the Poisson brackets. Therefore, any one of them can be chosen. The possible combinations are presented in Table I. While these schemes are free from “global” errors,

TABLE I. Decomposition table of symplectic integrators.

A	$\frac{\tau}{4}$	$\frac{\tau}{2}$	$\frac{\tau}{4}$	τ	$\frac{\tau}{4}$	$\frac{\tau}{2}$	$\frac{\tau}{4}$
1	S	π	S	ϵ	S	π	S
2	S	ϵ	S	π	S	ϵ	S
3	π	ϵ	π	S	π	ϵ	π
4	π	S	π	ϵ	π	S	π
5	ϵ	π	ϵ	S	ϵ	π	ϵ
6	ϵ	S	ϵ	π	ϵ	S	ϵ

they are of course sensitive to “local” errors due to the finite value of the time step. It is also not at all obvious that all six can be implemented with comparable efficiency. It is therefore useful to study the numerical stability and efficiency of these different combinations in particular, as former studies in molecular dynamics [38] and magnetic molecular dynamics [39] showed, apparently, numerical differences between them.

A sampler of such a study is presented in Appendix B.

It is important to keep in mind that the one-step evolution operators for ϵ and π describe shifts of the corresponding tensor components, whereas the one-step evolution operator for S describes rotations. In the equations,

$$e^{\mathcal{L}_\epsilon \tau}(\boldsymbol{\epsilon}(t), \boldsymbol{\pi}(t), \mathbf{S}(t)) = (\boldsymbol{\epsilon}(t) + \tau \dot{\boldsymbol{\epsilon}}(t), \boldsymbol{\pi}(t), \mathbf{S}(t)), \quad (32)$$

$$e^{\mathcal{L}_\pi \tau}(\boldsymbol{\epsilon}(t), \boldsymbol{\pi}(t), \mathbf{S}(0)) = (\boldsymbol{\epsilon}(t), \boldsymbol{\pi}(t) + \tau \dot{\boldsymbol{\pi}}(t), \mathbf{S}(t)), \quad (33)$$

$$e^{\mathcal{L}_S \tau}(\boldsymbol{\epsilon}(t), \boldsymbol{\pi}(t), \mathbf{S}(t)) = (\boldsymbol{\epsilon}(t), \boldsymbol{\pi}(t), \underbrace{\mathbf{S}(t + \tau)}_{R(\tau)\mathbf{S}(t)}), \quad (34)$$

where $\mathbf{S}(t + \tau) = R(\tau)\mathbf{S}(t)$ is given by Rodrigues’ rotation formula [40] for a spin vector around a given rotation vector $\tilde{\boldsymbol{\omega}}(t)$ where each of its components is $\tilde{\omega}_I(t) = \omega_I(t) - \frac{2}{\hbar} B_{JKL}^{(1)} \epsilon_{JK}(t) S_L(t)$. These equations describe the phase space of one particle only. To describe the dynamics of a continuum, we must deduce the equations for many particles.

One way to generalize Eqs. (25) for the case of many particles, labeled by an index, $i = 1, \dots, N$, according to the conventions of the previous sections, is the following:

$$\dot{\epsilon}_{IJ}^i = [M_{IJKL}^{(1)}]^{-1} \pi_{KL}^i, \quad (35)$$

$$\dot{\pi}_{IJ}^i = -V_0 C_{IJKL}^i \epsilon_{KL}^i + V_0 \sigma_{IJ}^{i \text{ ext}} - B_{IJKL}^i S_K^i S_L^i, \quad (36)$$

$$\dot{S}_I^i = \epsilon_{IJK} \left(\omega_J^i - \frac{2}{\hbar} B_{ABJC}^{(1)i} \epsilon_{AB}^i S_C^i \right) S_K^i. \quad (37)$$

The case of a staggered AF state is treated simply by letting $N = 2$. To simplify the mechanical part further, we can impose additional conditions pertaining to the uniformity of the external stress, mechanical constants, mass matrices, and magnetoelastic constants at each site. In what follows, we shall use the following *Ansatz*:

$$\begin{aligned} B_{IJKL}^{(1)1} &= B_{IJKL}^{(1)2}, \\ C_{IJKL}^1 &= C_{IJKL}^2, \\ M_{IJKL}^1 &= M_{IJKL}^2, \\ \sigma_{IJ}^{1 \text{ ext}} &= \sigma_{IJ}^{2 \text{ ext}}. \end{aligned} \quad (38)$$

The conservative part of the precession contains a local field, which is modified to include the antiferromagnetic exchange between the sites and a single anisotropy axis \mathbf{n} with an intensity K . One has

$$\omega_I^i = \frac{1}{\hbar} \sum_{(ij)} J^{ij} S_I^j + \frac{K}{\hbar} n_J s_J^i n_I. \quad (39)$$

Because of the exchange field, the Liouville operators for different spins do not commute either. A global geometric integrator, implementing the approach of Omelyan [41], which remains accurate up to third order in the time-step expansion, must therefore be constructed.

For any given time step, τ , the corresponding expression for the evolution operator, reads

$$e^{\mathcal{L}_S \tau} = e^{\mathcal{L}_{S^1} \frac{\tau}{2}} e^{\mathcal{L}_{S^2} \tau} e^{\mathcal{L}_{S^1} \frac{\tau}{2}} + O(\tau^3). \quad (40)$$

For $N = 2$, this operator is numerically identical to the operator obtained by permuting the site indices, $1 \leftrightarrow 2$.

The same reasoning is applied for the Liouville operators for the elastic variables that enter in Eqs. (26), and the corresponding global geometric integrators are constructed along the same lines. The system is then integrated by following one of the schemes displayed in Table I.

With these tools, we can study a plethora of phenomena that are sensitive to the coupling of magnetic, electric, and elastic degrees of freedom. In the following section, we shall apply this formalism for studying “fast switching” effects of the magnetization in antiferromagnetic media. The numerical accuracy ensured by the geometric integrators is necessary to describe picosecond switching times.

V. ANTIFERROMAGNETIC ULTRAFAST SWITCHING UNDER STRESS

In this section, we shall apply the formalism constructed above to describe how it is possible to generate and manipulate picosecond switching of the magnetization induced by STTs from a short pulse of electric current in elastic media that exhibit staggered AF order. Such a fast switching process in AFs is schematically displayed in Fig. 1 and can be realized, in practice, by a femtosecond laser excitation of the magnetic moments that generate a field-induced STT on the two sublattices. During the pulse, energy is transferred from conduction electrons to the sublattice magnetic moments

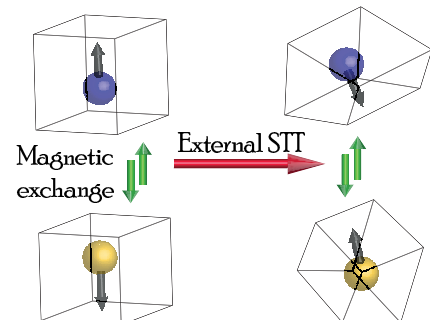


FIG. 1. Switching scheme for the antiferromagnetic magnetomechanically coupled toy model with external STT.

via STT (this is how the electric current affects the magnetic response), and hence it contributes to the exchange energy between the moments since local moments can be canted non-collinearly. The energy due to the strong exchange interaction between neighboring moments, which is commonly found in AFs, in particular due to magnetic anisotropy, appears as an effective inertia to the motion, leading to the appearance of a time scale much longer than that of the excitation pulse. Afterward, the system follows a natural path along the easy plane to circumvent the unfavorable anisotropy barrier and finally relaxes to a new magnetic configuration. The resulting dynamics is a switching of the two sublattice moments to the opposite direction through the easy plane.

This process defines the ultrafast antiferromagnetic switching effect. During the process, the Néel vector, which probes the difference between the magnetic moments of the two sublattices, acquires a net value that can be transferred as a so-called “spin accumulation” to an adjacent nonmagnetic normal material in order to pump the produced spin current via scattering of electrons. The reverse mechanism can be realized as well.

What was not considered before is the possibility to enhance or inhibit such a switching depending on tensile or compression effects, which are generated by an external stress. This stress couples to the internal strain produced by the intrinsic magnetoelastic interaction in such materials, as depicted in Fig. 1.

To conform to the notation used in our previous studies [15], Eq. (37) is supplemented with a nonconservative part, labeled T , on the right-hand side, which includes both a transverse damping and a damping-like STT torque,

$$T_I^i = \alpha \epsilon_{IJK} S_J^i S_K^i + G(s_J^i p_J - p_I s_J^i s_J^i). \quad (41)$$

The resulting equations of motion are numerically integrated using the approach of Sec. V. It is noteworthy that this equation also describes the “backreaction” of the magnetic response on the spin-transfer torque. On the other hand, we do not consider how this backreaction affects the current pulse itself, which is assumed to be external.

In Figs. 2 and 3 we report the evolution of the average magnetization $\mathbf{m} \equiv \frac{1}{2}(\mathbf{S}^1 + \mathbf{S}^2)$ and the Néel vector $\mathbf{l} \equiv \frac{1}{2}(\mathbf{S}^1 - \mathbf{S}^2)$, in the presence as well as the absence of magnetoelastic coupling, for a moderate external stress of $\sigma_{xx} = -2\mu_0 M_s^2$. We start the simulations using an initial configuration in which spins are aligned along the \hat{x} axis in an antiferromagnetic configuration, and we apply two 10 ps electric pulses of 0.0034 rad THz intensity, each separated by 50 ps, in the $\mathbf{p} = \hat{z}$ direction. In addition to the exchange interaction, the spins are subjected to a global anisotropy along the $\mathbf{n} = \hat{x}$ axis. The numerical value for α in the following studies is 0.005.

In the absence of magnetoelastic coupling, our results are identical to those of Cheng *et al.* [14] and to those we obtained under the same conditions in our previous work [15].

In the presence of magnetoelastic coupling, however, as the mechanical system is undamped, the results are quite different. Because of the presence of a constant stress, a finite mass matrix, and nonzero elastic constants, the mechanical system is expected to be oscillating freely, which is indeed

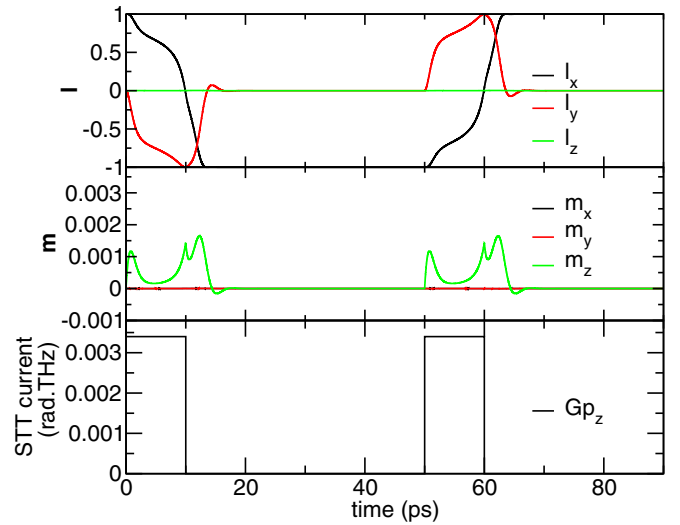


FIG. 2. Néel order parameter (upper panel) and average magnetization components (middle panel) for uncoupled switching. $\{K = 2\pi$ rad GHz, $\omega_E = 172.16$ rad THz, $M_s = 5 \times 10^5$ A m $^{-1}$ }. Initial conditions: $\{s^1(0) = -s^2(0) = \hat{x}\}$. The lower panel displays the STT pulses. The figures agree with Ref. [14] because the magnetoelastic constants are set to zero.

observed in Fig. 4, where we display the evolution of the strain components over time. Indeed, as one can see in Figs. 3 and 4, the characteristic oscillations of the mechanical system have repercussions on the Néel order parameter dynamics. This is even more striking for the spin accumulation, which is more than doubled by the coupling to the strain; here as well, the mechanical oscillations are reflected on the magnetic dynamics. What is interesting is that these characteristic mechanical oscillations are expected to be related to the sound velocity of the medium [42], which is controlled by the constants M_0

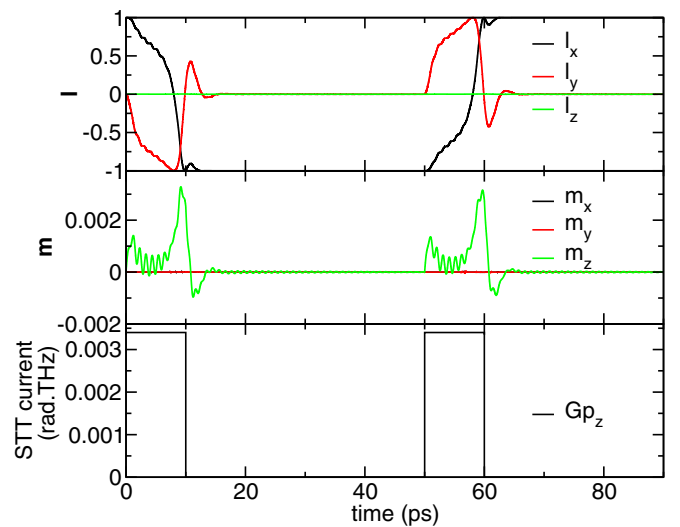


FIG. 3. Néel order parameter (upper panel) and average magnetization components (middle panel) for a coupled switching. $\{K = 2\pi$ rad GHz, $\omega_E = 172.16$ rad THz, $M_s = 5 \times 10^5$ A m $^{-1}$ }. Initial conditions: $\{s^1(0) = -s^2(0) = \hat{x}, \epsilon_{IJ}^i(0) = 0\}$. The lower panel displays the STT pulses. Here $B_0^{(1)} = 7.7\mu_0 M_s^2$ and $B_1^{(1)} = -23\mu_0 M_s^2$.

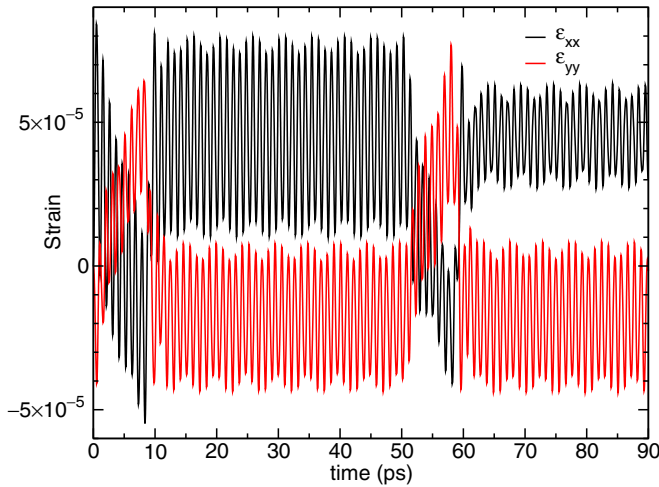


FIG. 4. Strain components as a function of time with the magnetoelastic constants turned on with parameters identical to Fig. 3.

and M_1 . In the present study, we have chosen $M_0 = 0$ and $M_1 = 10\,000$, but there should be a way to obtain these coefficients of the mass matrix more efficiently in order to describe these oscillations more accurately from experimentally easily accessible data. This, however, is not the focus of the present study, and it shall be studied more thoroughly elsewhere. As a consequence of such a stress-induced strain, the switching time of the magnetization is slightly faster and the amplitude of the magnetization is enhanced, depending on the values of the stress and magnetoelastic constants, as depicted in Fig. 3. We observe that a compression in one direction becomes tensile in the other one and vice versa depending on the sign of $B_1^{(1)}$. Conversely, if $B_1^{(1)}$ is of the opposite sign, a tensile stress would slow the switching process down.

This leads to another interesting question: How is the switching time affected by the values taken by either $B_0^{(1)}$ and $B_1^{(1)}$? We have verified that changing $B_0^{(1)}$ has no influence on it because this coefficient does not enter in the precession equation. It simply produces the Joule magnetostriction phenomena as anticipated before in Ref. [7]. However, changing $B_1^{(1)}$ has a strong influence. Figure 5 displays the switching time as a function of the values of varying $B_1^{(1)}$. By defining R as the ratio of $B_1^{(1)}$ divided by its natural value in NiO, we perform different simulations and report the time when the Néel vector x -component crosses over to negative values. One can see that this time decreases by increasing $B_1^{(1)}$, which makes sense as this is amplifying the effects of the tensile stress. When R becomes lower than 1, the effect is opposite. One aspect that is surprising, however, is that there is a quick drop of the switching time for approximately four times the value of $B_1^{(1)}$ over its natural value in NiO. This is due to the oscillations of the magnetization induced by the elastic coupling. As this coupling becomes stronger, one of the mechanical oscillatory peaks dips below 0 and thus the switching time appears to drop in a discontinuous fashion. This is another interesting consequence of the interplay of the magnetization and the strain, which could be captured in real experiments.

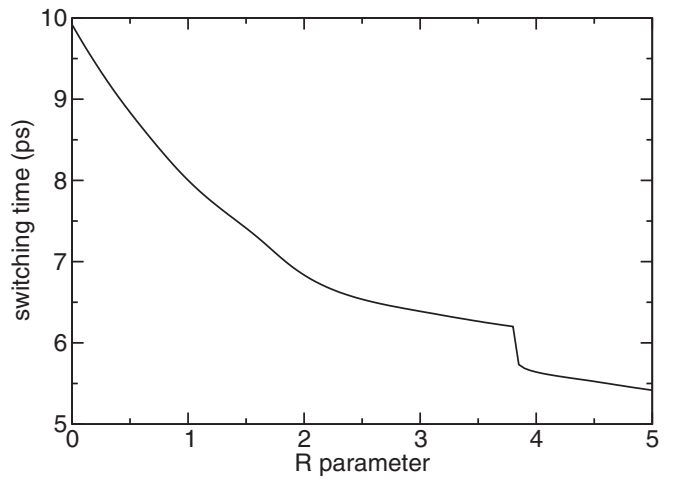


FIG. 5. Switching time (in ps) as a function of varying $B_1^{(1)}$ over its natural value in NiO.

VI. DISCUSSION AND CONCLUSIONS

In the present paper, we have set up a Hamiltonian framework for the consistent coupling between magnetic and elastic degrees of freedom. We have shown how the phase space, the Poisson bracket, and the Hamiltonian itself can be defined, and how the resulting equations of motion can be solved using symplectic integration schemes. We discuss the merits and weaknesses of several ways of splitting the integration, which is useful for selecting the most suitable scheme. We have focused in particular on the advantage of expressing the magnetic degrees of freedom using anticommuting variables in order to describe more directly the terms that can contribute to the coupling between magnetic and elastic degrees of freedom.

A linear coupling already describes nontrivial effects, which can be measured in real and numerical experiments, as we have shown. Indeed, in the case of NiO, we have shown that a small tensile stress can enhance the switching speed for the Néel order parameter. Furthermore, due to the characteristic oscillations, which are induced by the coupling to the strain, the switching speed appears to drop discontinuously, with increasing stress, when a peak of the oscillations of the Néel order parameter dips below zero, which triggers the switching. This switching leaves a characteristic imprint on the mechanical oscillations, i.e., a “backreaction,” for which our approach can fully account. Our approach thus provides a starting point for designing future antiferromagnetic devices for spintronics (as well as “straintronics”) applications, which are sensitive to both mechanical and magnetic effects.

The spin-transfer-torque sources, introduced in the Hamiltonian to describe the switching, also lead to damped oscillations for the magnetic degrees of freedom. This can serve as a starting point for taking into account stochastic effects more generally. The appropriate framework for purely magnetic degrees of freedom has already been set up [43], and we plan to report on how to take into account elastic degrees of freedom in future work.

ACKNOWLEDGMENTS

T.N. acknowledges financial support through a joint doctoral fellowship CEA-Région Centre under Grant No. 201600110872.

All authors contributed equally to this manuscript.

APPENDIX A: MODEL FOR PRECESSION THROUGH ANTICOMMUTING VARIABLES

We review some issues when dealing with classical spin variables, and we explain some limitations that are met by using the framework of commuting variables [44]. A common starting point to build precessional models is choosing the appropriate representation of the $\text{su}(2)$ algebra.

In the Heisenberg picture, the Ehrenfest theorem implies that the equations of motion for the average of the spin operator \hat{S} components read

$$i\hbar \frac{d\langle \hat{S} \rangle}{dt} = \langle [\hat{S}, \mathcal{H}] \rangle, \quad (\text{A1})$$

where \mathcal{H} is the Zeeman Hamiltonian operator for an external magnetic field \mathbf{H} such that

$$\mathcal{H} = -g\mu_0\mu_B \hat{S} \cdot \mathbf{H}. \quad (\text{A2})$$

From the commutation relations $[\hat{S}_i, \hat{S}_j] = i\epsilon_{ijk}\hat{S}_k$, one can quite straightforwardly show that

$$\frac{d\langle \hat{S} \rangle}{dt} = \frac{g\mu_B\mu_0}{\hbar} \langle \hat{S} \rangle \times \mathbf{H}, \quad (\text{A3})$$

which corresponds to the well-known Larmor precession of the expectation value of the spin in an external magnetic field \mathbf{H} .

Interestingly, a different—but equivalent—approach can be followed by considering the Majorana representation in terms of anticommuting variables, $\xi_I, \xi_I\xi_J + \xi_J\xi_I = 0$ [22] of the vector \mathbf{S} :

$$S_I = -\frac{i}{2}\epsilon_{IJK}\xi_J\xi_K, \quad (\text{A4})$$

which can easily be shown to commute as $S_I S_J = 0$. This last relation is of course not satisfactory. It can be easily avoided, however, by imposing that the ξ_I satisfy the anticommutation relations $\{\xi_I, \xi_J\} = \delta^{ij}$ —that they generate a Clifford algebra (up to a constant normalization) [23].

These relations imply that the S_I define a spin- $\frac{1}{2}$ representation of the $\text{su}(2)$ algebra. Higher spin representations can be defined by multilinear combinations [13], which are relevant for describing magnetic properties of composite objects; since we can work with the S_I instead of the ξ_I , however, this complication will not affect us here.

This representation highlights that the spin degrees of freedom, S_I , are in fact “composite” objects and that the “fundamental degrees of freedom” are the ξ_I . Therefore, it is useful to develop the description of the dynamics directly in terms of the ξ_I themselves. We shall recall the salient features below.

The Poisson brackets for the anticommuting variables ξ_I are related to those of S_I so that the dynamics will indeed be equivalent, in a way that was set forth many years ago, through the construction of a corresponding graded Poisson

bracket, which generalizes Poisson brackets from manifolds to supermanifolds [13].

In terms of any functions of anticommuting variables ξ , this bracket reads

$$\{f(\xi), g(\xi)\}_{\text{PB}} \equiv \frac{i}{\hbar} f(\xi) \overleftarrow{\frac{\partial}{\partial \xi_K}} \overrightarrow{\frac{\partial}{\partial \xi_K}} g(\xi), \quad (\text{A5})$$

with the corresponding definition of the left and right derivative of any function of the anticommuting variables. One can show that this bracket, also known as the “antibracket” of any two functions on a flat supermanifold, satisfies all necessary properties for a graded bracket, namely the (graded) Leibniz rule, (graded) antisymmetry, and (graded) Jacobi identity [45].

By taking this graded Poisson bracket for any two of these anticommuting variables, we get

$$\{\xi_I, \xi_J\}_{\text{PB}} = \frac{i}{\hbar} \delta_{IJ}. \quad (\text{A6})$$

This implies that any two such variables are canonically conjugate, since $\{\xi_I, -i\hbar\xi_J\}_{\text{PB}} = \delta_{IJ}$, and $\pi_I \equiv -i\hbar\xi_I$ defines the canonical conjugate [13].

By using the Grassmann properties of ξ , one proves that

$$\{S_I, S_J\}_{\text{PB}} = \frac{1}{\hbar} \epsilon_{IJK} S_K, \quad (\text{A7})$$

which is a consistency check that the S_I as defined in (A4) do realize a representation of the rotation group [24].

In Eq. (A5), if the functions of the ξ are chosen to contain only quadratic terms, then one can identify the previous bracket as a regular Poisson bracket on a Riemannian manifold for the commuting variables \mathbf{S} ,

$$\begin{aligned} \{f(\mathbf{S}), g(\mathbf{S})\}_{\text{PB}} &= \frac{i}{\hbar} \frac{\partial f}{\partial S_I} S_I \overleftarrow{\frac{\partial}{\partial \xi_K}} \overrightarrow{\frac{\partial}{\partial \xi_K}} S_J \frac{\partial g}{\partial S_J} \\ &= \{S_I, S_J\}_{\text{PB}} \frac{\partial f}{\partial S_I} \frac{\partial g}{\partial S_J} = \frac{1}{\hbar} \epsilon_{IJK} S_K \frac{\partial f}{\partial S_I} \frac{\partial g}{\partial S_J}, \end{aligned} \quad (\text{A8})$$

which is precisely the “spinning part” of the bracket introduced by Yang and Hirschfelder [34] for magnetized fluid dynamics, which reads

$$\{A, B\}_{\text{PB}} \equiv \frac{\partial A}{\partial q_I} \frac{\partial B}{\partial p_I} - \frac{\partial A}{\partial p_I} \frac{\partial B}{\partial q_I} - \frac{1}{\hbar} \epsilon_{IJK} S_I \frac{\partial A}{\partial S_J} \frac{\partial B}{\partial S_K}. \quad (\text{A9})$$

Similar expressions have already been found by Casalbuoni long ago [13] without having attracted the attention they deserve. Following the inverse path of canonical quantization, we use this graded Poisson bracket on any commuting quantity, which allows us to compute directly

$$\{\mathbf{S}, \mathcal{H}\}_{\text{PB}} = \frac{g\mu_B\mu_0}{\hbar} \mathbf{S} \times \mathbf{H}, \quad (\text{A10})$$

thereby highlighting that the description of \mathbf{S} in terms of ξ is an equivalent description of the dynamics.

For any time-dependent commuting functions of $\mathbf{S}(t)$, we can use this Poisson bracket to deduce a Liouville equation,

$$\frac{dF(\mathbf{S}(t))}{dt} = \{F(\mathbf{S}(t)), \mathcal{H}\}_{\text{PB}}. \quad (\text{A11})$$

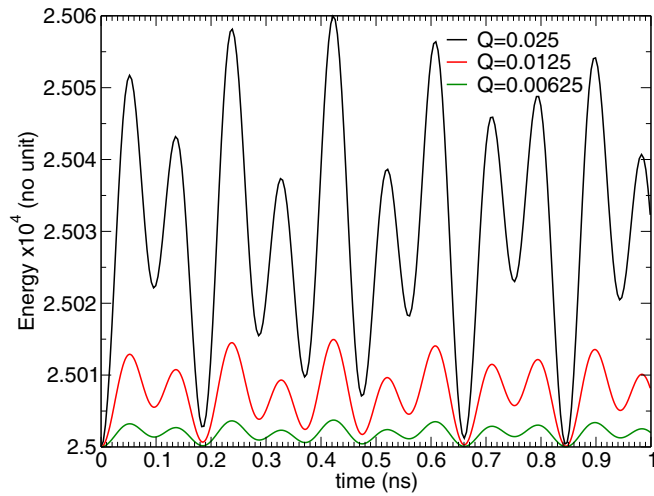


FIG. 6. Single-site total energy as a function of both time and variable time step Q . Conditions of the simulation are expressed in reduced units: $2C_0/\mu_0M_s^2 = 5.1 \times 10^5$, $2C_1/\mu_0M_s^2 = 3.5 \times 10^5$, $M_1V_0\mu_0M_s^2/2\hbar^2 = 1000$, $\omega_{DC} = (0, 0, 2\pi)$ rad GHz, $\pi_{11}(0) = 1$, $s(0) = (1, 0, 0)$. All the other parameters not reported, including initial conditions, are zero.

Consequently, the equations of motion for the variables ξ read much more simple expressions as

$$\frac{d\xi(t)}{dt} = \{\xi, \mathcal{H}\}_{PB} = \frac{i}{\hbar} \frac{\partial \mathcal{H}}{\partial \xi}, \quad (\text{A12})$$

which are known to form a nonrelativistic pseudoclassical mechanics [13].

One reason why using the representation of S in terms of ξ is useful is that it is intrinsically difficult to build a Lagrangian model for the commuting spin variable S , since its canonically conjugate variable cannot be unambiguously identified. As is well known by now, the conjugate of the dynamical variable ξ is proportional to itself [46]. Therefore, the dynamics of spinning degrees of freedom can be described, either through a vector of commuting variables on a curved manifold, or by a vector of anticommuting variables on a flat—though non-Riemannian—manifold. Finally, it has been found that the Majorana-fermion representation of $\frac{1}{2}$ -spin operators is also a powerful tool to straightforwardly compute spin-spin correlators [47], which represents an advantage for computing magnetic response functions in many-body systems.

APPENDIX B: NUMERICAL ACCURACY OF THE SPLITTING ALGORITHMS

The accuracy of the numerical schemes represented in Table I depends on the relative amplitude of the velocity terms ($\dot{\xi}$, $\dot{\pi}$, \dot{S}), and it can be monitored by checking the stability of

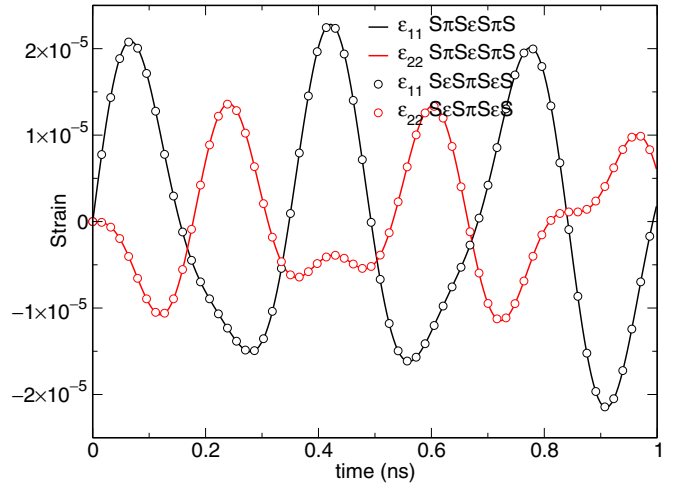


FIG. 7. Single-site strain components as a function of time for various numerical schemes. Conditions of the simulation are identical to those for Fig. 6, and the results are produced for $Q = 0.0025$ only.

Eq. (20) over time [36,37]. Figure 6 displays the total energy in one domain [given by the sum of Eqs. (21) and (22)] upon varying the numerical precision. The splitting algorithm considered corresponds to the label $A = 1$ in Table I. The numerical precision is controlled by the “quality factor,” chosen at the beginning of the simulation, which produces variable time steps τ according to the relation $\tau = Q/\|\omega\|$. Simulation conditions produce a total energy equal to $\pi_{11}^2(0)/4M_1$, which has to stay constant over time. We observe that this is indeed the case regardless of the value of the quality factor Q . We remark that, as $Q \rightarrow 0$, the variations about the average value of the energy are suppressed, as should be expected.

Figure 7 displays some of the nonvanishing components of the strain tensor over time [here $\varepsilon_{22}(t) = \varepsilon_{33}(t)$, and this third component is not reported] when using different splitting algorithms among those displayed in Table I. We observe less than 1% of a numerical relative difference between the two algorithms on the strain and its conjugate variables, and no difference (up to the machine precision) on the magnetization with a “coarse” quality factor Q , which cannot be detected by visual inspection in the figure. This difference falls to 0.1% when the quality factor is divided by 4. The same procedure can be repeated for all the splitting combinations in Table I. The conclusions previously drawn apply also for the magnetization, strain, and its conjugate variable, depending on the frequency of appearance of the split operator.

As expected, once a splitting algorithm is selected, the more frequently an operator is evaluated, the smaller is the error, although of course the time required also grows. This opens the possibility to select optimally a proper splitting algorithm, depending on the relative intensity of $\dot{\varepsilon}_{ij}$, $\dot{\pi}_{ij}$, \dot{S}_i over time.

[1] I. Radu, K. Vahaplar, C. Stamm, T. Kachel, N. Pontius, H. Dürr, T. Ostler, J. Barker, R. Evans, R. Chantrell *et al.*,

Nature (London) **472**, 205 (2011); T. Jungwirth, X. Marti, P. Wadley, and J. Wunderlich, *Nat. Nanotech.* **11**, 231 (2016).

- [2] J. Železný, P. Wadley, K. Olejník, A. Hoffmann, and H. Ohno, *Nat. Phys.* **14**, 220 (2018).
- [3] H. Ahmad, J. Atulasimha, and S. Bandyopadhyay, *Sci. Rep.* **5**, 18264 (2015).
- [4] H. Yan, Z. Feng, S. Shang, X. Wang, Z. Hu, J. Wang, Z. Zhu, H. Wang, Z. Chen, H. Hua, W. Lu, J. Wang, P. Qin, H. Guo, X. Zhou, Z. Leng, Z. Liu, C. Jiang, M. Coey, and Z. Liu, *Nat. Nanotech.* **14**, 131 (2019).
- [5] M. Fiebig, *J. Phys. D* **38**, R123 (2005).
- [6] J. Atulasimha and S. Bandyopadhyay, *Appl. Phys. Lett.* **97**, 173105 (2010).
- [7] E. Du Trémolet de Lacheisserie, *Magnetostriction: Theory and Applications of Magnetoelasticity* (CRC, Boca Raton, FL, 1993).
- [8] G. A. Maugin, *Continuum Mechanics of Electromagnetic Solids*, North Holland Series in Applied Mathematics and Mechanics No. 33 (North Holland, Amsterdam, 1988).
- [9] C. Kittel, *Rev. Mod. Phys.* **21**, 541 (1949).
- [10] N. Buiron, L. Hirsinger, and R. Billardon, *Le J. Phys. IV* **9**, Pr9 (1999).
- [11] L. Daniel and N. Galopin, *Eur. Phys. J.: Appl. Phys.* **42**, 153 (2008).
- [12] C. C. Mei and B. Vernescu, *Homogenization Methods for Multiscale Mechanics* (World Scientific, Singapore, 2010).
- [13] R. Casalbuoni, *Il Nuovo Cimento A (1965-1970)* **33**, 115 (1976); **33**, 389 (1976); F. Berezin and M. Marinov, *Ann. Phys.* **104**, 336 (1977); D. F. Nelson and B. Chen, *Phys. Rev. B* **50**, 1023 (1994).
- [14] R. Cheng, M. W. Daniels, J.-G. Zhu, and D. Xiao, *Phys. Rev. B* **91**, 064423 (2015).
- [15] T. Nussle, P. Thibaudeau, and S. Nicolis, *J. Magn. Magn. Mater.* **469**, 633 (2019).
- [16] H. B. G. Casimir, *Rev. Mod. Phys.* **17**, 343 (1945); L. D. Landau, E. M. Lifshitz, and L. D. Landau, *Theory of Elasticity*, 3rd ed., Course of Theoretical Physics Vol. 7 (Elsevier, Amsterdam, 2008).
- [17] B. K. D. Gairola, *Phys. Status Solidi B* **85**, 577 (1978); *Nonlocal Continuum Field Theories*, edited by A. C. Eringen (Springer, New York, 2004).
- [18] R. A. Toupin and B. Bernstein, *J. Acoust. Soc. Am.* **33**, 216 (1961); E. R. Callen and H. B. Callen, *Phys. Rev.* **129**, 578 (1963); W. F. Brown, *Magnetoelastic Interactions*, english ed., edited by C. Truesdell, R. Aris, L. Collatz, G. Fichera, P. Germain, J. Keller, M. M. Schiffer, and A. Seeger, Springer Tracts in Natural Philosophy Vol. 9 (Springer, Berlin, 1966).
- [19] G. Rosen, *Am. J. Phys.* **40**, 683 (1972).
- [20] H. F. Tiersten, *J. Math. Phys.* **5**, 1298 (1964); A. Akhiezer, V. Bar'yakhtar, and S. Peletminskii, *Spin Waves*, North Holland Series in Low Temperature Physics Vol. 1 (North Holland, Amsterdam, 1968).
- [21] D. Dever, *J. Appl. Phys.* **43**, 3293 (1972).
- [22] F. Wilczek, *Nat. Phys.* **5**, 614 (2009); J. Alicea, *Rep. Prog. Phys.* **75**, 076501 (2012).
- [23] P. Lounesto, *Clifford Algebras and Spinors*, 2nd ed., London Mathematical Society Lecture Note Series No. 286 (Cambridge University Press, Cambridge, 2003).
- [24] D. A. Varshalovich, A. N. Moskalev, and V. K. Khersonskii, *Quantum Theory of Angular Momentum* (World Scientific, Singapore, 1988).
- [25] R. F. Evans, W. J. Fan, P. Chureemart, T. A. Ostler, M. O. Ellis, and R. W. Chantrell, *J. Phys.: Condens. Matter* **26**, 103202 (2014).
- [26] O. Eriksson, A. Bergman, L. Bergqvist, and J. Hellsvik, *Atomistic Spin Dynamics: Foundations and Applications*, 1st ed. (Oxford University Press, Oxford, 2017).
- [27] J. H. van Vleck, *Phys. Rev.* **52**, 1178 (1937); L. Néel, *J. Phys. Radium* **15**, 225 (1954); E. W. Lee, *Rep. Prog. Phys.* **18**, 184 (1955).
- [28] R. F. Sabiryanov and S. S. Jaswal, *Phys. Rev. Lett.* **83**, 2062 (1999).
- [29] H. A. Kastrup, *Phys. Rep.* **101**, 1 (1983); I. V. Kanatchikov, [arXiv:hep-th/9312162](https://arxiv.org/abs/hep-th/9312162).
- [30] R. Arnowitz, S. Deser, and C. W. Misner, *Phys. Rev.* **117**, 1595 (1960).
- [31] S. A. Hojman, K. Kuchař, and C. Teitelboim, *Ann. Phys.* **96**, 88 (1976).
- [32] R. Hill, *Proc. R. Soc. London A* **314**, 457 (1970).
- [33] J. Kijowski and W. Szczyrba, *Commun. Math. Phys.* **46**, 183 (1976); W. Szczyrba, *ibid.* **51**, 163 (1976); J. E. Marsden, R. Montgomery, P. J. Morrison, and W. B. Thompson, *Ann. Phys.* **169**, 29 (1986).
- [34] K.-H. Yang and J. O. Hirschfelder, *Phys. Rev. A* **22**, 1814 (1980).
- [35] R. Skomski, *Simple Models of Magnetism*, Oxford Graduate Texts (Oxford University Press, Oxford, 2008).
- [36] S. Blanes, F. Casas, J. A. Oteo, and J. Ros, *Phys. Rep.* **470**, 151 (2009).
- [37] E. Hairer, C. Lubich, and G. Wanner, *Geometric Numerical Integration: Structure-Preserving Algorithms for Ordinary Differential Equations*, 2nd ed., Springer Series in Computational Mathematics (Springer-Verlag, Berlin Heidelberg, 2006).
- [38] P. F. Batcho and T. Schlick, *J. Chem. Phys.* **115**, 4019 (2001).
- [39] D. Beaujouan, P. Thibaudeau, and C. Barreteau, *Phys. Rev. B* **86**, 174409 (2012).
- [40] O. Rodrigues, *J. Math. Pures Appl.* **5**, 380 (1840); J. Honerkamp and H. Römer, *Theoretical Physics: A Classical Approach* (Springer, Berlin, 1993); P. Thibaudeau and D. Beaujouan, *Physica A* **391**, 1963 (2012).
- [41] I. P. Omelyan, I. M. Mryglod, and R. Folk, *Comput. Phys. Commun.* **151**, 272 (2003).
- [42] R. W. Ogden, *Non-Linear Elastic Deformations*, dover ed., Dover Books on Physics (Dover, Mineola, NY, 1997).
- [43] J. Tranchida, P. Thibaudeau, and S. Nicolis, *Phys. Rev. E* **98**, 042101 (2018).
- [44] L. Brink, P. Di Vecchia, and P. Howe, *Phys. Lett. B* **65**, 471 (1976). *Nucl. Phys. B* **118**, 76 (1977).
- [45] J. Gomis, J. París, and S. Samuel, *Phys. Rep.* **259**, 1 (1995); I. V. Kanatchikov, *Rep. Math. Phys.* **40**, 225 (1997).
- [46] R. Casalbuoni, *Phys. Lett. B* **62**, 49 (1976).
- [47] A. Shnirman and Y. Makhlin, *Phys. Rev. Lett.* **91**, 207204 (2003); W. Mao, P. Coleman, C. Hooley, and D. Langreth, **91**, 207203 (2003); P. Schad, Y. Makhlin, B. N. Narozhny, G. Schön, and A. Shnirman, *Ann. Phys.* **361**, 401 (2015).